RESEARCH ARTICLE

TBI Server: A Web Server for Predicting Ion Effects in RNA Folding

Yuhong Zhu[1], Zhaojian He[2], Shi-Jie Chen[3]*

1 Department of Physics, Department of Biochemistry, and Informatics Institute, University of Missouri, Columbia, MO 65211, USA; Department of Physics, Hangzhou Normal University, Hangzhou, Zhejiang 310036, China, 2 Department of Physics, Department of Biochemistry, and Informatics Institute, University of Missouri, Columbia, MO 65211, USA, 3 Department of Physics, Department of Biochemistry, and Informatics Institute, University of Missouri, Columbia, MO 65211, USA

* chenshi@missouri.edu

Abstract

Background

Metal ions play a critical role in the stabilization of RNA structures. Therefore, accurate prediction of the ion effects in RNA folding can have a far-reaching impact on our understanding of RNA structure and function. Multivalent ions, especially Mg^{2+}, are essential for RNA tertiary structure formation. These ions can possibly become strongly correlated in the close vicinity of RNA surface. Most of the currently available software packages, which have widespread success in predicting ion effects in biomolecular systems, however, do not explicitly account for the ion correlation effect. Therefore, it is important to develop a software package/web server for the prediction of ion electrostatics in RNA folding by including ion correlation effects.

Results

The TBI web server http://rna.physics.missouri.edu/tbi_index.html provides predictions for the total electrostatic free energy, the different free energy components, and the mean number and the most probable distributions of the bound ions. A novel feature of the TBI server is its ability to account for ion correlation and ion distribution fluctuation effects.

Conclusions

By accounting for the ion correlation and fluctuation effects, the TBI server is a unique online tool for computing ion-mediated electrostatic properties for given RNA structures. The results can provide important data for in-depth analysis for ion effects in RNA folding including the ion-dependence of folding stability, ion uptake in the folding process, and the interplay between the different energetic components.

Introduction

Because RNA backbone is highly negatively charged, the folding of RNA requires counterions to neutralize the backbone charge and to reduce Coulomb repulsion. As a result, RNA folding is sensitive to the ionic condition, such as ion type, size, valence and concentration [1–12]. The interaction between counterions (metal ions) and RNA plays a critical role in RNA folding, including the structure and the folding stability and folding kinetics [13–15]. Accurate evaluation of the ion electrostatic effect is essential for the prediction of RNA folding.

One of the challenges in modeling the ion effects is how to treat the potentially important ion correlation and fluctuation effects. Coulomb interaction is a long-range force. As a result, the electric force acting on an ion is a function not only of the its own coordinates but also of the simultaneous positions of the other ions. In an ionic solution, ions have a strong tendency to accumulate in the close vicinity of (the negatively charged) RNA. The ions could reach high local density which leads to ion correlation. One of the resultant effects from ion correlation is the coupling between the ion binding events at the different sites. Such a coupling effect is stronger for multivalent ions than monovalent ions due to their higher charges. Motivated by the importance to treat ion correlation effects, especially for multivalent ions such as Mg^{2+} ions, which are essential for the stabilization of RNA tertiary structure, we developed the Tightly Bound Ion (TBI) model [16–20]. To treat the correlation effect inevitably requires the consideration of the ensemble of discrete many-ion distributions instead of a mean-field distribution. Thus, the TBI model can also account for the fluctuations in ion distribution.

The TBI model is a theory for predicting ion-dependent RNA folding stability [16–20]. The model was first reported in 2005 [16] and further developed in 2008 [17] with explicit inclusion of the solvent polarization effect through the Generalized Born model. In 2012 [20], with an energy landscape-guided approach for the sampling of ion distribution, the model undergoes a significant improvement with a drastically enhanced computational efficiency. The enhanced version of the TBI allows us to treat RNAs of sequences longer than 80 nucleotides. For example, with enhanced version of the model, the computational time of a Tetraloop-receptor system of 81 nucleotides is about 30–80 minutes for the different ionic conditions [21]. Tests of the TBI predictions against the experimental data for ion binding properties and ion-dependent folding stabilities (Table 1.) [17–19, 22] suggested that the TBI model may be reliable for predicting ion effects in RNA folding.

Table 1. Comparison between the TBI and the Poisson-Boltzmann predictions and test against experimental data.

RNA or DNA	Comparison of parameters	Reference	The average error for BP	The average error for TBI
Three DNA helices	Folding free energy	Fig. 2d [22]	1.2 kcal/mol	0.1 kcal/mol
Two DNA helices	Melting temperature	Fig. 5 [23]	5.4°C	1.0°C
Two RNA helices	Ion binding Fraction	Fig. 2a [23]	0.11	0.06
24bp B-DNA helix	Ion binding Fraction	Fig. 2a [24]	0.08	0.01
40bp A-RNA helix	Ion binding Fraction	Fig. 2c [24]	0.15	0.04
40bp B-DNA helix	Ion binding Fraction	Fig. 2e [24]	0.12	0.03
BWYV pseudoknot RNA	Ion binding Fraction	Fig. 3a [24]	0.05	0.03
58-nt rRNA	Ion binding Fraction	Fig. 3c [24]	0.10	0.03
Yeast tRNA^{Phe}	Ion binding Fraction	Fig. 3e [24]	0.06	0.03

doi:10.1371/journal.pone.0119705.t001

Methods

The Tightly Bound Ion (TBI) model

We classify the ions into two types according to their Coulomb correlation strengths: The tightly bound ions (of strong correlation) and the diffusive ions (of weak correlation). The region (a thin layer around the RNA surface) where the tightly bound ions are distributed is called the tightly bound region. For an N-nt RNA, the tightly bound region can be divided into N cells, each around a phosphate. For the tightly bound ions, we sample the discrete modes of ion distribution. Here a mode is defined by the number of bound ions in the cells. Through enumeration of the discrete ion binding modes and evaluation of the multi-ion electrostatic energy for each mode, the TBI model accounts for the correlation between the bound ions and the fluctuation of ion distributions [16–19, 23, 24].

For a given ion binding mode M, ions are allowed to move inside the respective cells. By sampling the coordinates of the tightly bound ions within their respective cells (dR_i below), we calculate the partition function Z_M of the system:

$$Z_M = Z^{(id)} \left(\frac{N_Z}{V} \right)^{N_b} \left(\int \prod_{i=1}^{N_b} dR_i \right) e^{-\Delta G_M / k_B T}, \tag{1}$$

where $Z^{(id)}$ is the partition function for the uniform ion solution (without the RNA), N_Z is the total number of z-valent counterions and V is the volume of the solution, N_b and $\int \prod_{i=1}^{N_b} dR_i$ are the number and the volume integral for the tightly bound ions, respectively, and ΔG_M is the free energy of the system for mode M.

Electrostatic free energy for each mode

The electrostatic energy for the charges inside the tightly bound region is computed as the sum of the self-energy ΔU_{self}, the polarization energy ΔU_{pol}, and the Coulomb energy ΔU_{ele}:

$$\Delta U_{self} = \frac{1}{2} \left(\frac{1}{\epsilon_w} - \frac{1}{\epsilon_{in}} \right) \sum_p \frac{q_p^2}{B_i} + \left(\frac{1}{\epsilon_w} - \frac{1}{\epsilon_{in}} \right) \sum_i \frac{q_i^2}{2} \left(\frac{1}{B_i} - \frac{1}{B_i^0} \right)$$

$$\Delta U_{pol} = \left(\frac{1}{\epsilon_w} - \frac{1}{\epsilon_{in}} \right) \sum_{m<n} \frac{q_m q_n}{\sqrt{r_{mn}^2 + B_m B_n \exp \left(-\frac{r_{mn}^2}{4 B_m B_n} \right)}}$$

$$\Delta U_{ele} = \sum_{m<n} \frac{q_m q_n}{\epsilon_{in} r_{mn}} \tag{2}$$

where Σ_p, Σ_i, Σ_{mn} are the summations over the phosphates, tightly bound ions, and both, respectively, and q_p, q_i, $q_m q_n$ are the respective charges. r_{mn} is the distance between m and n, B_x is the Born radius of x, B_i^0 is the radius of the hydrated ion, and ϵ_{in} (~ 12) and ϵ_w (~ 78 at room temperature) are the dielectric constants of RNA and water, respectively. ϵ_w is given by

$$\epsilon_w(T) = 87.740 - (0.4008) \, T + (9.398 \times 10^{-4}) \, T^2 - (1.41 \times 10^{-6}) \, T^3, \tag{3}$$

where T is the temperature in Celsius.

The free energy of the diffusive ions is calculated as the sum of the enthalpic ΔU_d and entropic $-T\Delta S_d$ terms:

$$\Delta U_d = \frac{1}{2}\int \sum_\alpha c_\alpha(\mathbf{r})z_\alpha q[\Psi(\mathbf{r}) + \Psi'(\mathbf{r})]d^3\mathbf{r}$$

$$\Delta S_d = -k_B \int \sum_\alpha \left[c_\alpha(\mathbf{r}) \ln \frac{c_\alpha(\mathbf{r})}{c_\alpha^0} - c_\alpha(\mathbf{r}) + c_\alpha^0 \right] d^3\mathbf{r} \tag{4}$$

where c_α is the concentration of ion species α, c_a^0 is the bulk concentration, $\Psi(r)$ and $\Psi'(r)$ are the electrostatic potentials with and without the diffusive ions, respectively. The electric potentials are determined from the Poisson-Boltzmann equation with the presence of the tightly bound ions.

For a given mode M, the ensemble average over the positions of the tightly bound ions, denoted as $\langle \ldots \rangle$, gives the electrostatic free energy components: $\Delta G_M = \langle \Delta U_{self} + \Delta U_{pol} + \Delta U_{ele} + \Delta U_d - T\Delta S_d \rangle$.

Free energy components

Averaging over all the tightly bound ion distribution modes gives the electrostatic free energy of the system:

$$\Delta G_{tot} = -k_B T \ln \sum_M (Z_M/Z^{(id)}). \tag{5}$$

The probability of mode M is $P_M = e^{-(\Delta G_M - \Delta G_{tot})/k_B T}$.

The weighted sum over all the modes gives the free energy components:

- Coulomb free energy $\Delta E_{ele} = \Sigma_M \langle \Delta U_{ele} \rangle P_M$

- Polarization free energy $\Delta G_{pol} = \Sigma_M \langle \Delta U_{pol} \rangle P_M$

- Self-polarization free energy $\Delta G_{self} = \Sigma_M \langle \Delta U_{self} \rangle P_M$

- Entropic free energy $\Delta G_s = \Delta G_{tot} - (\Delta E_{ele} + \Delta G_{pol} + \Delta G_{self})$

Here the entropic free energy ΔG_s includes the entropy of the diffusive ions and the (combinatorial) entropy of the tightly bound ions.

Binding fraction

The TBI model [23, 24] gives the mean binding fraction of Na$^+$ and Mg^{2+} ions on each nucleotide i:

$$f_{Mg^{2+}}^{(i)} = \bar{f}_b^{(i)} + \frac{1}{N}\int \left[c_{Mg^{2+}}(\mathbf{r}) - c_{Mg^{2+}}^0 \right] d^3\mathbf{r} \tag{6}$$

$$f_{Na^+} = \frac{1}{N}\int \left[c_{Na^+}(\mathbf{r}) - c_{Na^+}^0 \right] d^3\mathbf{r} \tag{7}$$

where N is the number of the nucleotides in RNA and $\bar{f}_b^{(i)}$ is the average binding fraction of the tightly bound Mg^{2+} ions on nucleotide i:

$$\bar{f}_b^{(i)} = \sum_M N_b^{(i)} P_M \tag{8}$$

where $N_b^{(i)}$ is the number of the bound ions on the ith nucleotide in ion binding mode M. We note the different expressions above for Mg^{2+} and Na^+ ions. This is because the monovalent ions (Na^+) are usually weakly correlated and do not exist in the form of tightly bound ions.

Results

Input

The TBI server predicts the electrostatic thermodynamic properties for a given RNA structure. The server has a simple input interface (see Fig. 1). The input parameters include the temperature, the monovalent/divalent ion concentrations, and the RNA structure. The current version of the TBI server allows only Na^+ and Mg^{2+} ions. The server accepts the standard PDB format for the input RNA 3D structure. The user can paste the PDB file into the text window for the input structure. To conveniently identify the submitted jobs, user has the option to define the job names. The user also has the option to retrieve the calculated results either through email (provided by the user) or from a webpage.

For example, to calculate the electrostatic free energy for T2 pseudoknot (PDB code: 2TPK [25], an RNA pseudoknot), we input the parameters as shown in Fig. 1a and the 3D structure of the RNA by pasting the text data of the 2TPK PDB file. We can choose to receive the calculated results through email with the job name and job ID (automatically generated by web server) shown in the subject line (see Fig. 1b)
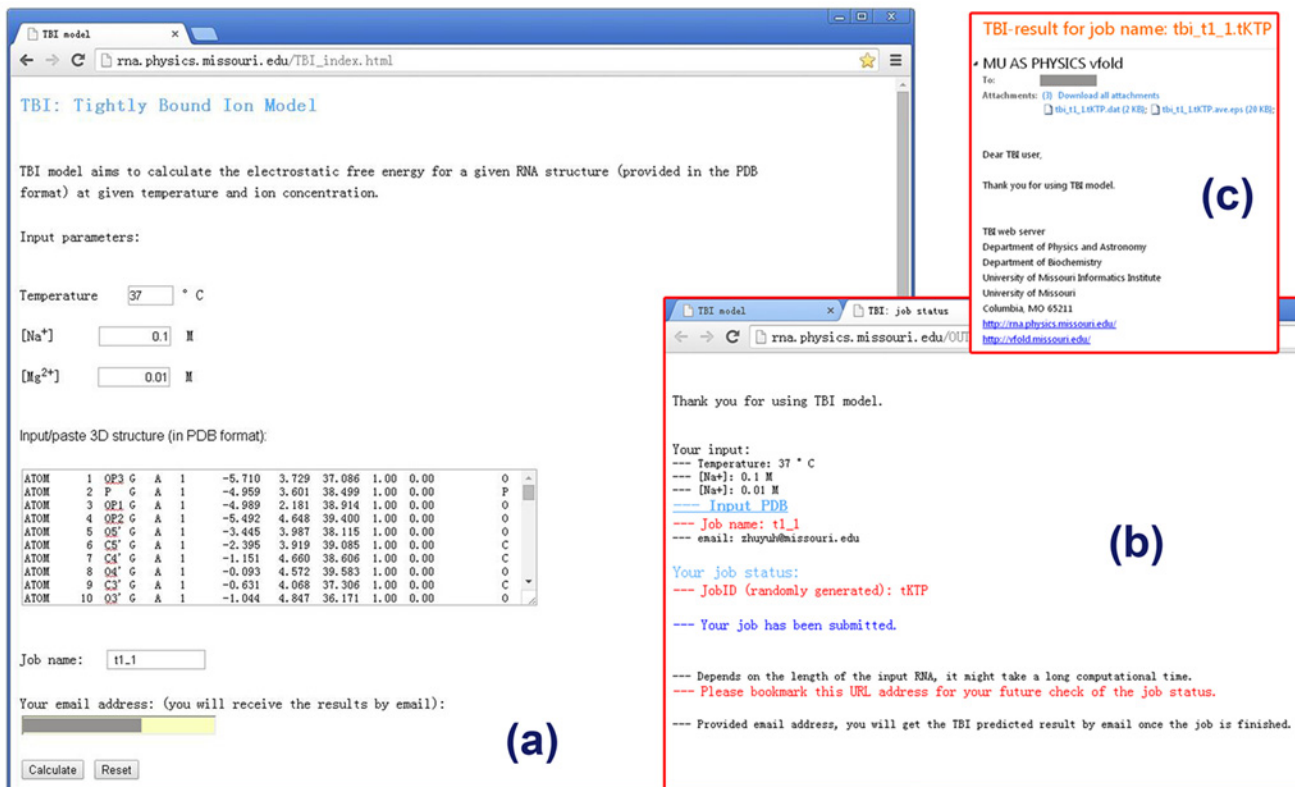

Fig 1. The user interface of the TBI server. (a) the job submission page, (b) the notification page, and (c) the result email.

Output

The results from the TBI server are presented in three output files, one text file and two figure files (see Fig. 1c). The text file (with filename extension ".dat") (shown in Fig. 2) shows the solution condition (input parameters) and the numerical results of the predicted fractional bound ions and the free energies.

In the output data file, the first column is the index number of the nucleotides, and the third and the fifth column are the average ion binding fraction for each nucleotide (Equations 6 & 7) and the most probable binding mode (the mode M of the lowest free energy ΔG_M) [16], respectively. For example, the number "1" in the fifth column means that the corresponding nucleotide has one tightly bound Mg^{2+} ion in the most probable ion binding mode, while the number "0" means there is no tightly bound Mg^{2+} bound to the nucleotide in the most probable mode. The ion binding properties are shown diagrammatically in the two output figure files, which give the mean (see Fig. 3) and the most probable ion binding modes, respectively (see Fig. 4).

The data file also gives the total electrostatic free energy ΔG_{tot} and the free components: the self-polarization energy ΔG_{self}, the polarization energy ΔG_{pol}, the Coulomb energy ΔE_{ele}, and the entropic free energy ΔG_s. The units of the (free) energies are $k_B T$.

Examples of usage

Example 1: Basic calculations with the TBI server. Here, we show the basic usage of the TBI server through a simply example (shown in Fig. 5). The first step is to input the parameters and the RNA structure data (PDB code: 2TPK [25]) (see Fig. 5-step1). We then provide the job name and a valid email address if we choose to receive the results via email notification. We can simply leave the email address blank if we choose to retrieve the results from a webpage. In this example, we use "T2_test" for the job name. We then click "Calculate" to submit the job. The calculated results will be send to user provided email address (see Fig. 5 step2) or shown on the webpage for download when the calculations are finished. The three output files are "T2_test.*.dat", "T2_test.*.eps" and "T2_test.*.site.eps" for this example. The "T2_test.*.dat" file contains all the free energy and ion binding properties data, which can be used to predict ion-dependent folding stabilities (see Examples 2 and 3 below). The two figures show the profile of the average binding fractions for all the nucleotides (see Fig. 3 or Fig. 5-step 3a) and the most probability binding sites (see Fig. 4 or Fig. 5-step 3b). Fig. 5-step 4 shows the most probable Mg^{2+} ion binding mode for the T2 RNA pseudoknot. It is important to note that the most probable binding mode does not necessarily correspond to the specific ion binding sites observed in the structure determination experiment. This is because the current TBI model does not account for effects that may be important for specific ion binding such as ion dehydration and ion chelated interactions with specific chemical groups.

Example 2: Mg^{2+}-induced folding stability of T2 pseudoknot. To understand the ion-dependent folding stability of the T2 pseudoknot (see Example 1), we compute the ion-dependence of the free energy difference between the folded (pseudoknot) state and the intermediate (hairpin) state [19, 26, 27]. For the purpose of free energy calculation, previous studies suggested a computationally efficient method by using an effective 24-nt helix to represent the hairpin conformational ensemble [19, 26, 27]. We input the two structures (the effective helix and the pseudoknot; see Figs. 6ab) into the TBI server and compute the free energies at the different Mg^{2+} ion concentrations.

According to the thermodynamic cycle of RNA folding and $[Mg^{2+}]$ ion binding [26–29], we calculate the Mg^{2+}-induced folding stability $\Delta\Delta G_{Mg^{2+}}$ from the following equation:

$$\Delta\Delta G_{Mg^{2+}} = \Delta G^F_{Mg^{2+}} - \Delta G^I_{Mg^{2+}} = [\Delta G(F \cdot Mg^{2+}) - \Delta G^F_o] - [\Delta G(I \cdot Mg^{2+}) - \Delta G^I_o], \qquad (9)$$

```
* * * * * * * * * * * * * * * *
*                              *
*    The  solution   condition *
*                              *
* * * * * * * * * * * * * * * *


T (Celsius)   37.000
Na+           0.10000 M
Mg2+          0.01000 M




* * * * * * * * * * * * * * * *
*                              *
*    The calculated results    *
*                              *
* * * * * * * * * * * * * * * *


                mean        most
nucleotide    binding     probable
              fraction    binding
    1           0.100       0.000
    2           0.420       0.000
    3           0.609       0.000
    4           0.386       0.000
    5           0.756       0.000
    6           1.003       1.000
                . . .
                . . .
   35           0.027       0.000
   36           0.020       0.000

f_Mg            0.287
f_Na            0.267

G_tot  (in kT)    79.787
G_pol  (in kT)     4.739
E_ele  (in kT)    40.588
G_s    (in kT)    34.460
G_self (in kT)  -131.165
```

Fig 2. An example for the result text file. The file includes two parts: the solution condition and the calculated results.

doi:10.1371/journal.pone.0119705.g002
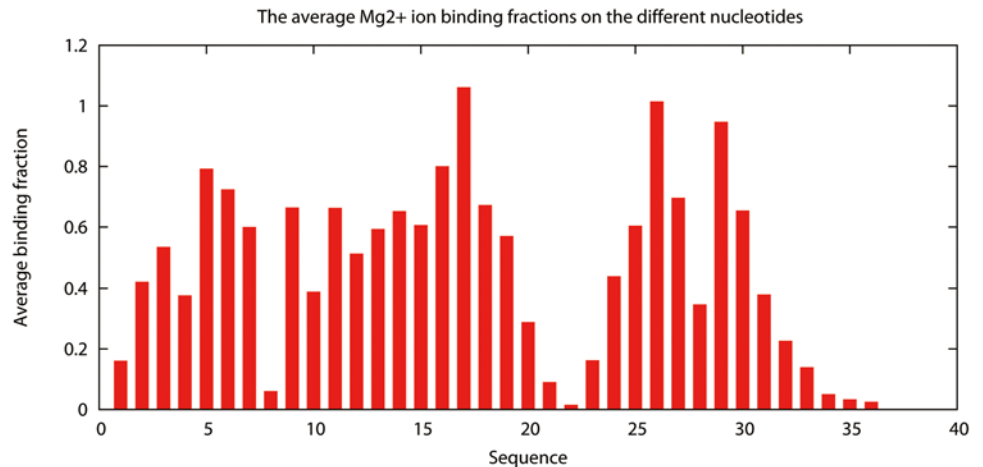
Fig 3. The average binding fraction. The average binding fraction on each nucleotide of the T2 RNA pseudoknot in 10mM Mg^{2+} and 100 mM Na$^+$ at T = 37°C.

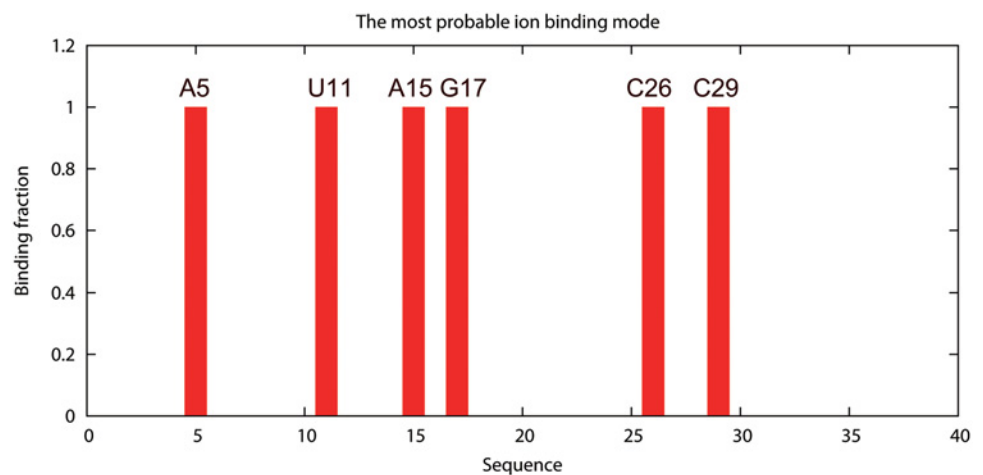doi:10.1371/journal.pone.0119705.g003

Fig 4. The most probable binding mode for the tightly bound ions. The lowest energy ion binding mode for the T2 RNA pseudoknot at [Mg^{2+}] = 10mM, [Na$^+$] = 100mM, T = 37°C. The most probable binding sites (nucleotides) are denoted with the orange color in the inset.

doi:10.1371/journal.pone.0119705.g004

where, $\Delta G_{\text{Mg}^{2+}}^F$ and $\Delta G_{\text{Mg}^{2+}}^I$ are the Mg^{2+}-caused electrostatic free energy differences for the folded and the intermediate states [18, 26, 27], respectively, $\Delta G(F \cdot \text{Mg}^{2+})$ and ΔG_o^F are the electrostatic free energies of the folded state with and without Mg^{2+} ions, respectively; $\Delta G(I \cdot \text{Mg}^{2+})$ and ΔG_o^I are the electrostatic free energies of the unfolded state with and without Mg^{2+} ions, respectively. The electrostatic free energies $\Delta G(F \cdot \text{Mg}^{2+})$ and ΔG_o^F for the folded state and $\Delta G(I \cdot \text{Mg}^{2+})$ and ΔG_o^I for the intermediate state can be calculated from the TBI server. To estimate $\Delta G(I \cdot \text{Mg}^{2+})$ and ΔG_o^I, we use a 24-nt helix [18, 26, 27]: for the electrostatic free energy calculation:

$$\Delta G(I) = \Delta G_{\text{helix}} \cdot \frac{N_I}{N_{\text{helix}}} = \Delta G_{\text{helix}} \cdot \frac{36}{24} \qquad (10)$$
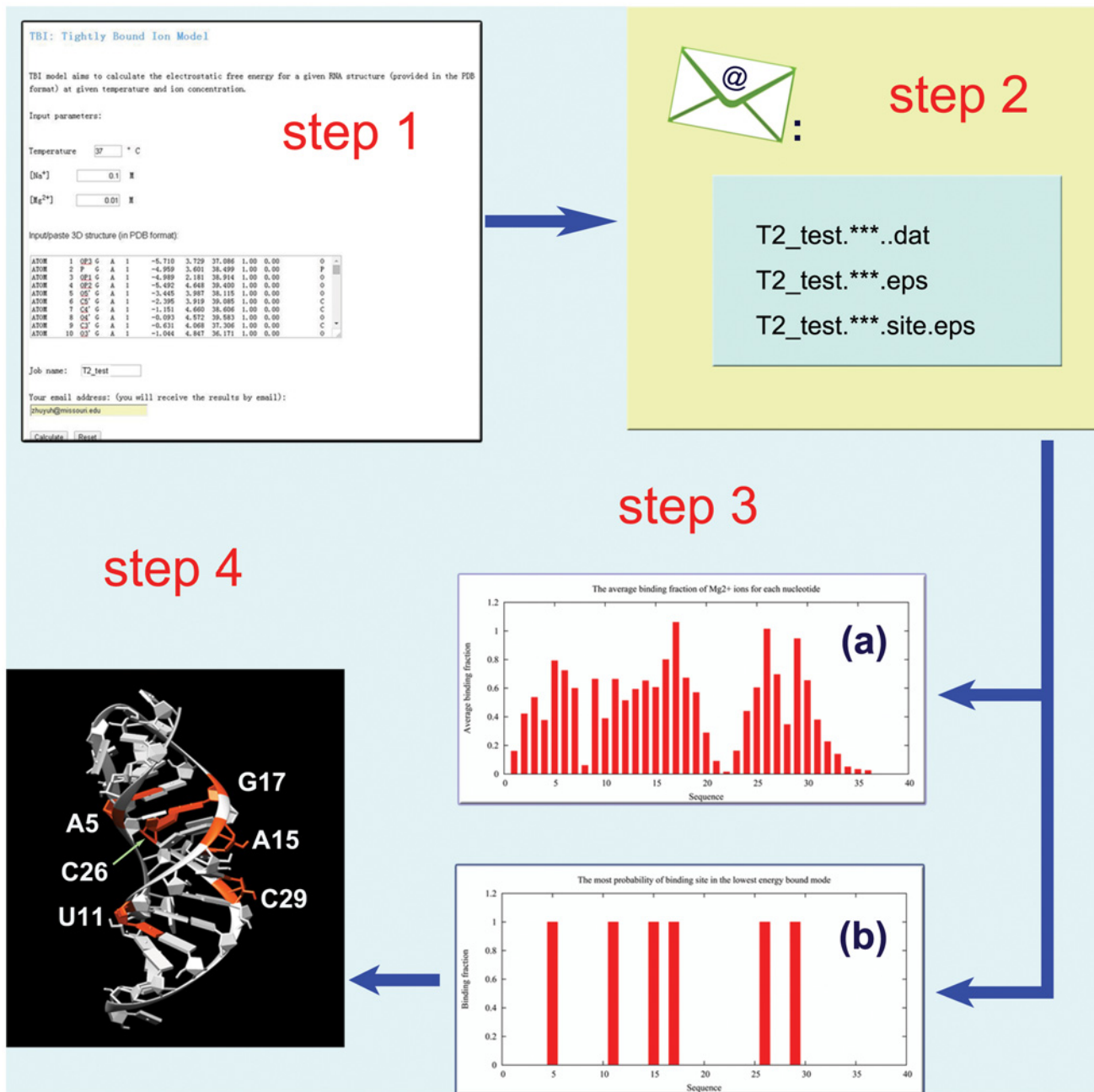
Fig 5. An example for the usage of the TBI server. The server computes the ion binding properties and the electrostatic free energies for T2 RNA (PDB code 2TPK [25]) in a solution with 10 mM Mg^{2+}, 100 mM Na$^+$, and $T = 37°$C.

doi:10.1371/journal.pone.0119705.g005

Here N_I (36) and N_{helix} (24) are the number of nucleotides of the T2 pseudoknot and the 24-nt helix, respectively. The calculated results are shown in the Table 2 and the curve of Mg^{2+}-induced folding stability is shown in Fig. 6c.

Example 3: Estimation of Mg^{2+} ion uptake. The uptake of ions is the increase in the number of bound ions in a process such as RNA structural change [30, 31]. The TBI server gives the average binding fraction of monovalent and divalent ions for a given RNA structure.
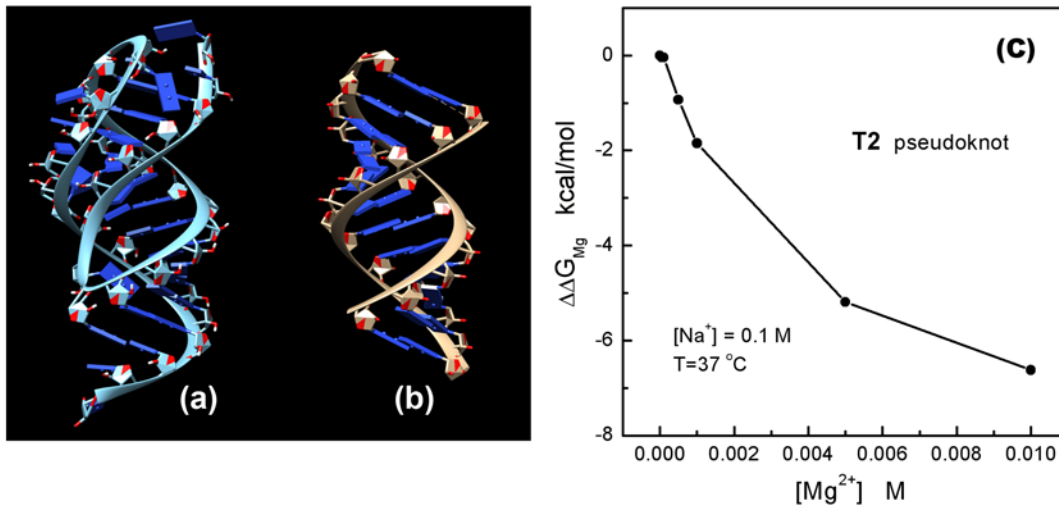
Fig 6. The Mg^{2+}-induced folding stability $\Delta\Delta G_{Mg^{2+}}$ for the T2 pseudoknot. (a) and (b) show the 3D structures of T2 pseudoknot (the folded state) and the 24-nt A-form helix, respectively; (c) shows the Mg^{2+}-induced folding stability.

doi:10.1371/journal.pone.0119705.g006

Table 2. The table shows the calculated electrostatic free energies of the T2 pseudoknot (the folded state, ΔG^F), the 24-nt helix (ΔG_{helix}) and the intermediate state (ΔG^I) under various [Mg^{2+}].

[Mg^{2+}] (in mol)	0	0.00005	0.0001	0.0005	0.001	0.005	0.01
ΔG^F (in kcal/mol)	59.52	59.47	59.45	58.41	57.27	51.64	47.28
ΔG_{helix} (in kcal/mol)	30.30	30.29	30.28	30.18	30.04	28.51	26.55
ΔG^I (in kcal/mol)	45.45	45.43	45.42	45.26	45.05	42.77	39.82

doi:10.1371/journal.pone.0119705.t002

The average uptake Mg^{2+} ions for the folding process can be estimated from the difference in binding fraction between the folded and the unfolded RNA [21, 30, 31]. Using T2 pseudoknot as an example, we estimate the Mg^{2+} uptake for the folding from the hairpin intermediate to the final pseudoknot state.

Since the ion binding distribution can be sensitive to the RNA structure, we need to generate explicitly the ensemble of discrete hairpin conformations [32–35]. This can be achieved by using a separate method such as molecular dynamics or Monte Carlo simulational method or a coarse-grained conformational sampling method. To the purpose of illustrate the electrostatic calculations, we use the lowest free energy T2 hairpin structure as an example. The structure is based on a conformational ensemble generated by molecular dynamics simulation [34, 35]. Using the TBI server, for the different Mg^{2+} ion concentrations, we can compute the Mg^{2+} ion binding fractions ($f_{Mg^{2+}}$) for the T2 pseudoknot and the hairpin, respectively. We then predict the Mg^{2+} ion uptake in the folding process from the hairpin to the pseudoknot. As shown in Fig. 7, with a fixed 0.1M Na$^+$ and increasing [Mg^{2+}] from 0 M to 5 mM, the Mg^{2+} ion uptake increases from 0 to 0.035 per nucleotide. Table 3 and Fig. 7 show the TBI-calculated binding fractions and the Mg^{2+} ion uptake curve as a function of [Mg^{2+}].

Conclusion

Accurate prediction of ion-mediated forces in the stabilization of RNA structure is critical to understanding RNA structure and function. Multivalent ions, especially Mg^{2+} ions, are crucial
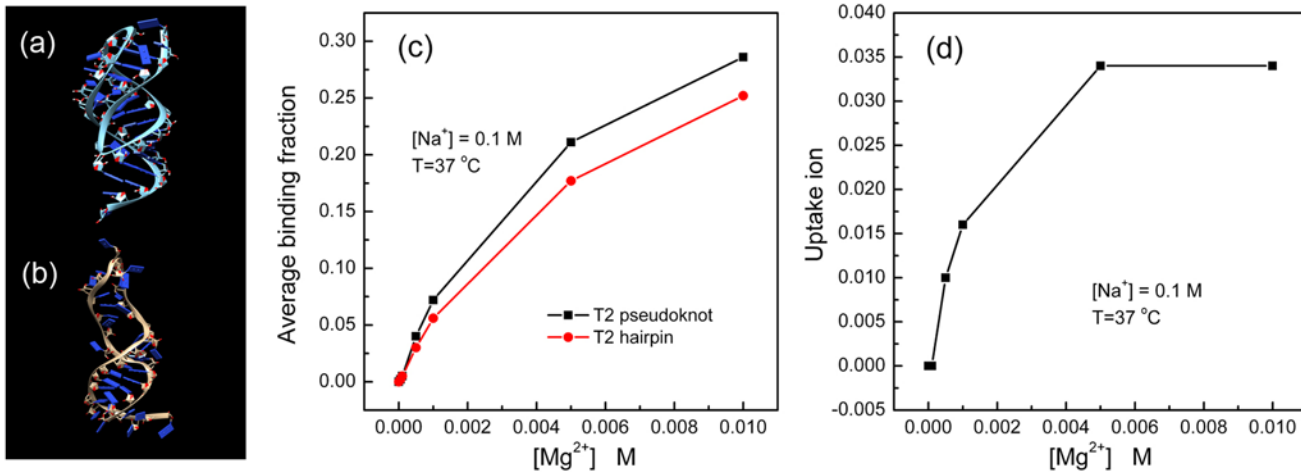
Fig 7. The binding fraction and the uptake of Mg^{2+} ions as a function of [Mg^{2+}]. (a) and (b) show the 3D structures of the T2 pseudoknot (the folded state) and T2 hairpin (the intermediate state), respectively; (c) shows the binding fraction curves for the T2 pseudoknot (black) and the hairpin (red). (d) shows the Mg^{2+} uptake as a function of [Mg^{2+}].

doi:10.1371/journal.pone.0119705.g007

Table 3. The table lists the calculated average binding fraction of the T2 pseudoknot (the folded state, f^F) and the intermediate state (f^I) under the different [Mg^{2+}] conditions.

[Mg^{2+}] (in mol)	0	0.00005	0.0001	0.0005	0.001	0.005	0.01
f^F	0	0.002	0.005	0.040	0.072	0.211	0.286
f^I	0	0.002	0.005	0.030	0.056	0.177	0.252

doi:10.1371/journal.pone.0119705.t003

for RNA tertiary structure folding. For the multivalent ions, ion correlation and fluctuation may play a important role in RNA folding. This demands a web server that can treat ion correlation and fluctuation effects in RNA folding. TBI is such a server. For a user provided RNA structure and ionic condition, the server computes ion binding properties, electrostatic free energies and various components. The TBI server provides results can be used to predict the ion-dependence of folding stability and ion uptake/release in the folding process. In the future development, we plan (a) to expand the server to treat other types of ions beyond the Mg^{2+} and Na$^+$ ions, (b) to use a more detailed charge distribution (such as partial charge) to model RNA charges, and (c) to include ion dehydration effects for ion binding.

Acknowledgments

Author Contributions

Conceived and designed the experiments: SJC. Performed the experiments: YZ ZH. Analyzed the data: YZ ZH SJC. Wrote the paper: YZ ZH SJC.

References

1. Bowman JC, Lenz TK, Hud NV, Williams LD. Cations in charge: magnesium ions in RNA folding and catalysis. Curr Opin Chem Biol. 2012; 22: 262–272.

2. Chen AA, Marucho MN, Baker A, Pappu RV. Simulations of RNA interactions with mono-valent ions. Meth Enzymol. 2009; 469: 411–432. doi: 10.1016/S0076-6879(09)69020-0 PMID: 20946801

3. Draper DE. A guide to ions and RNA structure. RNA. 2004; 10: 335–343. doi: 10.1261/rna.5205404 PMID: 14970378

4. Draper DE, Grilley D, Soto AM. Ions and RNA folding. Annu Rev Biophys Biomol Struct. 2005; 34: 221–243. doi: 10.1146/annurev.biophys.34.040204.144511 PMID: 15869389

5. Ha BY, Thirumalai D. Bending rigidity of stiff polyelectrolyte chains: A single chain and a bundle of multi-chains. Macromolecules. 2003; 36: 9658–9666. doi: 10.1021/ma021226k

6. Harris RC, Boschitsch AH, Fenley MO. Sensitivities to parameterization in the size-modified poisson-boltzmann equation. J Chem Phys. 2014; 140: 075102. doi: 10.1063/1.4864460 PMID: 24559370

7. Kirmizialtin S, Pabit SA, Meisburger SP, Pollack L, Elber R. RNA and its ionic cloud: Solution scattering experiments and atomically detailed simulations. Biophys J. 2012; 102: 819–828. doi: 10.1016/j.bpj.2012.01.013 PMID: 22385853

8. Leipply D, Lambert D, Draper DE. Ion-RNA interactions: thermodynamic analysis of the effects of mono- and divalent ions on RNA conformational equilibria. Meth Enzymol. 2009; 469: 433–463. doi: 10.1016/S0076-6879(09)69021-2 PMID: 20946802

9. Li Pan TX, Tinoco I. Mechanical unfolding of two DIS RNA kissing complexes from HIV-1. J Mol Biol. 2009; 386: 1343–1356. doi: 10.1016/j.jmb.2009.01.023 PMID: 19452632

10. Moghaddam S, Caliskan G, Chauhan S, Hyeon C, Briber RM, Thirumalai D, et al. Metal ion dependence of cooperative collapse transitions in RNA. J Mol Biol. 2009; 393: 753–764. doi: 10.1016/j.jmb.2009.08.044 PMID: 19712681

11. Qiu X, Giannini J, Howell SC, Xia Q, Ke F, Andresen K. Ion competition in condensed DNA arrays in the attractive regime. Biophys J. 2013; 105: 984–992. doi: 10.1016/j.bpj.2013.07.004 PMID: 23972850

12. Qiua XY, Parsegian VA, Rau DC. Divalent counterion-induced condensation of triple-strand DNA. Proc Natl Acad Sci U S A. 2010; 107: 21482–21486. doi: 10.1073/pnas.1003374107

13. Baker N, Holst M, Wang F. Adaptive Multilevel Finite Element Solution of the Poisson-Boltzmann Equation II: Refinement at Solvent-Accessible Surfaces in Biomolecular Systems. J Comput Chem. 2010; 21: 1343–1352. doi: 10.1002/1096-987X(20001130)21:15%3C1343::AID-JCC2%3E3.3.CO;2-B

14. Li L, Li C, Sarkar S, Zhang J, Witham S, Zhang Z, et al. DelPhi: a comprehensive suite for DelPhi software and associated resources. BMC Biophys. 2012; 5: 9. doi: 10.1186/2046-1682-5-9 PMID: 22583952

15. Hou TJ, Wang JM, Li YY, Wang W. Assessing the Performance of the MM/PBSA and MM/GBSA Methods. 1 The Accuracy of Binding Free Energy Calculations Based on Molecular Dynamics Simulations. J Chem Inf Model. 2011; 5: 69–82. doi: 10.1021/ci100275a

16. Tan ZJ, Chen S-J. Electrostatic correlations and fluctuations for ion binding to a finite length polyelectrolyte. J Chem Phys. 2005; 122: 44903. doi: 10.1063/1.1842059 PMID: 15740294

17. Tan ZJ, Chen S-J. Electrostatic free energy landscapes for dna helix bending. Biophys J. 2008; 94: 3137–3149. doi: 10.1529/biophysj.107.122366 PMID: 18192348

18. Tan ZJ, Chen S-J. Importance of diffuse metal ion binding to RNA. Met Ions Life Sci. 2011; 9: 101–124. doi: 10.1039/9781849732512-00101 PMID: 22010269

19. Tan ZJ, Chen S-J. Salt contribution to RNA tertiary structure folding stability. Biophys J. 2011; 101: 176–187. doi: 10.1016/j.bpj.2011.05.050 PMID: 21723828

20. He Z, Chen S-J. Predicting ioncnucleic acid interactions by energy landscape-guided sampling. J Chem Theory Comput. 2012; 8: 2095–2102. doi: 10.1021/ct300227a PMID: 23002389

21. He Z, Zhu Y, Chen S-J. Exploring the electrostatic energy landscape for tetraloop-receptor docking. Phys Chem Chem Phys. 2014; 16: 6367–6375. doi: 10.1039/c3cp53655f PMID: 24322001

22. Tan ZJ, Chen S-J. Nucleic acid helix stability: effects of salt concentration, cation valence and size, and chain length. Biophys J. 2006; 90: 1175–1190. doi: 10.1529/biophysj.105.070904 PMID: 16299077

23. Tan ZJ, Chen S-J. RNA helix stability in mixed Na^+/Mg^{2+} solution. Biophys J. 2007; 92: 3615–3632. doi: 10.1529/biophysj.106.100388 PMID: 17325014

24. Tan ZJ, Chen S-J. Predicting ion binding properties for RNA tertiary structures. Biophys J. 2010; 99: 1565–1576. doi: 10.1016/j.bpj.2010.06.029 PMID: 20816069

25. Holland JA, Hansen MR, Du ZH, Hofman DW. An examination of coaxial stacking of helical stems in a pseudoknot motif: The gene 32 messenger RNA pseudoknot of bacteriophage T2. RNA. 1999; 5: 257–271. doi: 10.1017/S1355838299981360 PMID: 10024177

26. Misra VK, Draper DE. The linkage between magnesium binding and RNA folding. J Mol Biol. 2002; 317: 507–521. doi: 10.1006/jmbi.2002.5422 PMID: 11955006

27. Misra VK, Shiman R, Draper DE. A thermodynamic framework for the magnesium-dependent folding of RNA. Biopolymers. 2003; 69: 118–136. doi: 10.1002/bip.10353 PMID: 12717727

28. Grilley D, Misra V, Caliskan G, Draper DE. Importance of partially unfolded conformations for Mg^{2+}-induced folding of RNA tertiary structure: Structural models and free energies of Mg^{2+} interactions. Biochemistry. 2007; 46: 10266–10278. doi: 10.1021/bi062284r PMID: 17705557

29. Woodson SA. Metal ions and RNA folding: a highly charged topic with a dynamic future. Curr Opin Chem Biol. 2005; 9: 104–109. doi: 10.1016/j.cbpa.2005.02.004 PMID: 15811793

30. Leipply D, Draper DE. Dependence of rna tertiary structural stability on Mg^{2+} concentration: interpretation of the hill equation and coefficient. Biochemistry. 2010; 49: 1843–1853. doi: 10.1021/bi902036j PMID: 20112919

31. Fiore JL, Holmstrom ED, Fiegland LR, Hodak JH, Nesbitt DJ. The role of counterion valence and size in GAAA tetraloop-receptor docking/undocking kinetics. J Mol Biol. 2012; 423: 198–216. doi: 10.1016/j.jmb.2012.07.006 PMID: 22796627

32. Schroeder R, Barta A, Semrad K. Strategies for RNA folding and assembly. Nat Rev Mol Cell Biol. 2004; 5: 908–919. doi: 10.1038/nrm1497 PMID: 15520810

33. Zhou HX. From induced fit to conformational selection: a continuum of binding mechanism controlled by the time scale of conformational transitions. Biophys J. 2010; 98: L15–7. doi: 10.1016/j.bpj.2009.11.029 PMID: 20303846

34. Xu XJ, Zhao PN, Chen S-J. Vfold: a web server for RNA structure and folding thermodynamics prediction. PLoS ONE. 2014; 9: e107504. doi: 10.1371/journal.pone.0107504 PMID: 25215508

35. Zhu Y, Chen S-J. Many-body effect in ion binding to RNA. J Chem Phys. 2014; 141: 055101. doi: 10.1063/1.4890656 PMID: 25106614